Advancements in Human Norovirus Cultivation in Human Intestinal Enteroids

Khalil Ettayebi[a], Gurpreet Kaur[a], Ketki Patil[a], Janam Dave[a], B. Vijayalakshmi Ayyar[a], Victoria R Tenge[a], Frederick H. Neill[a], Xi-Lei Zeng[a], Allison L. Speer[b], Sara C. Di Rienzi[a], Robert A. Britton[a], Sarah E. Blutt[a], Sue E. Crawford[a], Sasirekha Ramani[a], Robert L. Atmar[a,c], Mary K. Estes[a,c*]

[a]Department of Molecular Virology and Microbiology, Baylor College of Medicine (BCM), Houston, TX, USA

[b]Department of Pediatric Surgery, McGovern Medical School at the University of Texas Health Science Center at Houston (UTHealth), Houston, TX, USA

[c]Department of Medicine, BCM, Houston, TX, USA

Keywords: HuNoV cultivation, enteroids, organoids, organoid growth media

*Address correspondence to Mary K. Estes, mestes@bcm.edu

Abstract

Human noroviruses (HuNoVs) are a significant cause of both epidemic and sporadic acute gastroenteritis worldwide. The lack of a reproducible culture system for HuNoVs was a major obstacle in studying virus replication and pathogenesis for almost a half-century. This barrier was overcome with our successful cultivation of multiple HuNoV strains in human intestinal enteroids (HIEs), which has significantly advanced HuNoV research. We previously optimized culture media conditions and generated genetically-modified HIE cultures to enhance HuNoV replication in HIEs. Building upon these achievements, we now present additional advancements to this culture system, which involve testing different media, unique HIE lines, and additional virus strains. HuNoV infectivity was evaluated and compared in new HIE models, including HIEs generated from different intestinal segments of individual adult organ donors, HIEs made from human embryonic stem cell-derived human intestinal organoids that were transplanted into mice (H9tHIEs), genetically-engineered (J4*FUT2* knock-in [*KI*], J2*STAT1* knock-out [*KO*]) HIEs, as well as HIEs derived from a patient with common variable immunodeficiency (CVID) and from infants. Our findings reveal that small intestinal HIEs, but not colonoids, from adults, H9tHIEs, HIEs from a CVID patient, and HIEs from infants support HuNoV replication with segment and strain-specific differences in viral infection. J4*FUT2-KI* HIEs exhibit the highest susceptibility to HuNoV infection, allowing the cultivation of a broader range of GI and GII HuNoV strains than previously reported. Overall, these results contribute to a deeper understanding of HuNoVs and highlight the transformative potential of HIE cultures in HuNoV research.

Importance

Human noroviruses (HuNoVs) are very contagious and cause significant acute gastroenteritis globally, but studying them has been hindered by the lack of a reproducible culture system for nearly 50 years. This barrier was overcome by successfully cultivating multiple HuNoV strains in human intestinal enteroids (HIEs), advancing HuNoV research. We previously optimized culture conditions and developed genetically modified HIEs to enhance HuNoV replication. In this study, we tested different media, unique HIE lines, and additional virus strains, evaluating HuNoV infectivity in new HIE models. These models include HIEs from various intestinal segments of adult donors, human embryonic stem cell-derived HIEs transplanted into mice (H9tHIEs), genetically-engineered HIEs (J4*FUT2* knock-in [*KI*], J2*STAT1* knock-out [*KO*]), HIEs from a common variable immunodeficiency (CVID) patient, and from infants. Our findings show that adult small intestinal HIEs, H9tHIEs, CVID patient HIEs, and infant HIEs support HuNoV replication with segment and strain-specific differences. J4*FUT2-KI* HIEs exhibited the highest susceptibility, allowing cultivation of a broader range of HuNoV strains. These results enhance the understanding of HuNoVs and highlight the transformative potential of HIE cultures in HuNoV research.

Introduction

Human noroviruses (HuNoVs) are the most common cause of both epidemic and sporadic acute gastroenteritis worldwide. They also cause chronic infections in immunocompromised cancer and transplant patients and are a severe health burden for this population (1-3). Annually, HuNoV infections are responsible for 685 million cases of

diarrhea and over 212,000 deaths globally (4). In the United States alone, these infections lead to approximately 109,000 hospitalizations, generating a substantial economic impact of more than $10.6 billion in healthcare expenses and societal costs (4-6). Even though HuNoV was discovered in 1968, there are still no FDA-approved vaccines and efficacious therapeutics available, highlighting the challenges associated with combating these infections and the need for further research and development in this area (7, 8).

One of the main obstacles in studying and understanding HuNoVs was the absence of a culture system to effectively cultivate these viruses. However, in 2016, a significant breakthrough was achieved with the establishment of the human intestinal stem cell-derived enteroid (HIE) system for HuNoV cultivation (9). This development overcame a five-decade barrier in laboratory models for HuNoVs, opening new avenues for investigating HuNoV biology. Since the establishment of the HIE system, significant advancements have been made in unraveling various aspects of HuNoV biology, including strain-specific differences in replication, methods of virus inactivation, innate immune responses, antiviral susceptibility, and characterization of neutralizing antibodies (10-29). Here, we report further advancements in the HIE culture system by testing HuNoV infection in multiple unique HIE lines and expanding the profile of cultivatable HuNoV strains.

Results

We previously reported that differentiation of HIEs and infection carried out in the commercial IntestiCult™ Organoid Growth Medium (OGM) media from STEMCELL Technologies (formerly known as IntestiCult media) supports robust replication of HuNoV strains that replicated poorly in HIEs grown in our original in-house culture medium (23). A new IntestiCult™ Organoid Differentiation Medium (ODM) media (also from STEMCELL Technologies) became available in 2020, and we conducted a comparative analysis between OGM media and the new ODM media to assess their impact on HuNoV replication. For these studies, we used the previously reported genetically-modified J4*FUT2-KI* HIE line in which the fucosyltransferase 2 (*FUT2*) gene was knocked-in to the secretor negative J4 HIE (30). The J4*FUT2-KI* HIE line showed better HuNoV binding to the HIE cell surface and replication of several HuNoVs (30). J4*FUT2-KI* HIE monolayers, seeded in OGM and differentiated in either OGM or ODM media, were infected with GII.4 Sydney[P31] and GII.3[P21] HuNoV strains. Both media supported viral replication. However, replication of both strains was enhanced based on significant greater geometric mean $\log_{10}$ genome equivalents (GE) increases in virus yields from 1 hour post infection (hpi) to 24 hpi in HIEs plated using OGM media when compared to ODM media (Figure 1). Consequently, all subsequent experiments described in this study were executed using OGM media. Infections were conducted using the OGM differentiation medium supplemented with the bile acid sodium glycochenodeoxycholate (GCDCA), necessary for GII.3 infection and enhancing GII.4 infection (9).

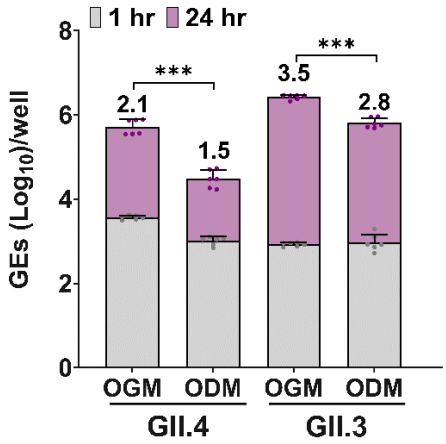

Figure 1: HuNoV replication is enhanced in HIEs plated in OGM compared to ODM media. 3D J4*FUT2/KI* HIEs were propagated in WRNE media. Monolayers were seeded in OGM proliferation medium with ROCK inhibitor and differentiated in OGM or ODM differentiation media. Differentiated monolayers were inoculated with GII.4 Sydney[P31] (9×10^5 GEs/well) or GII.3[P21] (4.3×10^5 GEs/well) diluted in CMGF(-) with 500 µM GCDCA. After 1 hpi, monolayers were washed twice and cultured in the OGM or ODM differentiation media (+ 500 µM GCDCA). Values on bars represent net $\log_{10}$ difference in viral growth (Δ24hr-1hr) preformed in triplicate. Gray shading indicates GE at 1 hpi and purple shows GE at 24 hpi. Asterisks indicate significant difference at 24 hpi between culture conditions. Error bars denote standard deviation (n=2). Data from one out of two experiments is presented. Each data bar corresponds to the mean derived from three wells of inoculated HIE monolayers. Total RNA extracted from each well was evaluated by RTqPCR in duplicate. *** p value < 0.001.

We next conducted a comparative investigation of viral replication using multiple unique HIE lines derived from various sources. We aimed to capture segment-specific and strain-specific differences in the susceptibility of HIE lines that may influence viral replication. We first evaluated HIEs generated from intestinal tissues obtained from four independent organ donors (designated 2002, 2003, 2004, and 2005). From each donor, four HIE lines were established, representing the three segments of the small intestine [duodenum (D), jejunum (J), and ileum (I)] as well as the colon (C). The HIE lines were confirmed to be secretor positive through genotyping assays for fucosyltransferase 2 (*FUT2*), which indicated their ability to express the histoblood group antigens (HBGAs) necessary for HuNoV infection. The susceptibility of HIE lines to HuNoV strains GII.4 Sydney[P31] and GII.3[P21] was assessed, focusing on segment-specific differences (Table 2).

Table 1: HuNoV replication in HIEs from four donors

	GII.4 / Sydney				GII.3			
HIEs	2002	2003	2004	2005	2002	2003	2004	2005
Duodenal	1.3 (*0.9-1.5*)	1.6 (*1.4-1.8*)	2.0 (*1.8-2.1*)	1.8 (*1.7-1.9*)	0.8 (*0.5-1.1*)	0	1.6 (*1.2-1.8*)	0.8 (*0.5-1.1*)
Jejunal	2.2 (*1.9-2.5*)	2.1 (*1.9-2.3*)	1.8 (*1.5-2.0*)	2.1 (*1.9-2.2*)	2.0 (*1.9-2.1*)	0	1.8 (*1.4-2.1*)	1.2 (*0.8-1.6*)
Ileal	2.2 (*2.1-2.4*)	2.2 (*2.1-2.4*)	1.6 (*1.5-1.9*)	2.7 (*2.5-2.8*)	1.8 (*1.4-2.2*)	0.1	1.4 (*1.2-1.6*)	0.5 (*0.3-0.8*)
Colonic	0	0	0	0	0	0	0	0

Differentiated monolayers were inoculated with GII.4 Sydney[P31] (9×10^5 GEs/well) or GII.3[P21] (4.3×10^5 GEs/well) diluted in CMGF(-) with 500 μM GCDCA. After 1 hpi, monolayers were washed twice and cultured in the OGM differentiation medium (+ 500 μM GCDCA). Values represent compiled data of net $\log_{10}$ geometric mean increase in viral growth (Δ24hpi-1hpi) from 3 experiments and six replicates. in each experiment; values in parentheses correspond to 95% confidence interval (95% CI).

GII.4 replication was observed across all small intestinal HIE lines. A 2-way ANOVA analysis, with Tukey's multiple comparisons test, showed no significant differences in viral replication [shown by Log_{10}(GE) increases] within small intestinal segments derived from the same donor or within the same segment of different donors (Table 1). GII.3 replication occurred in HIE lines generated from small intestinal segments of three out of the four donors (excluding 2003), with no significant differences in Log_{10}(GE) increases within small intestinal segments from the same donor. However, significant variations in viral replication were observed among HIEs of the same segment from various donors. None of the colonic HIE lines supported replication of either GII.3 or GII.4 HuNoV strains. These observations suggest that while small intestinal HIE lines are generally permissive to HuNoV infection, there may be variations in viral replication efficiency within different segments of the small intestine from various donors. The observed difference in infectivity between GII.4 and GII.3 HuNoV for HIEs from donor 2003 also indicates strain-specific differences in susceptibility to infection within the same donor that is independent of FUT2 expression. Further, these findings confirm our previous report of lack of replication in colonic lines derived from different independent

individuals (23), indicating segment-specific differences in the susceptibility of HIE lines to HuNoV infection.

In addition, we assessed HuNoV infection in other unique HIEs. First, we evaluated viral replication in HIEs generated from H9 human embryonic stem cells (H9hESC)-derived human intestinal organoids (HIOs) that were transplanted into immunocompromised mice for 8 weeks (referred in this paper as H9tHIEs). These H9tHIEs were derived from HIOs generated *in vitro* by directed differentiation of H9hESCs. HIOs contain both epithelial and mesenchymal cells (31). Previous RNASeq analyses of such HIOs showed these cultures exhibit a more fetal-like transcriptional expression pattern; they are therefore considered immature (32). However, *in vivo* transplantation of such HIOs into mice (tHIOs) can induce maturation of the intestinal epithelium resulting in tHIOs with a more adult-like transcriptional profile and enhanced levels of tight junction proteins (32-35). Additionally, the morphology and cellular maturation patterns in tHIOs are similar to fetal intestinal epithelial development (36). For example, an 8-week-old tHIO demonstrates proliferation confined to the crypts similar to a gestational week 18 human fetal intestine (36). To investigate whether matured tHIOs could be susceptible to HuNoV infection, we transplanted immature HIOs under the kidney capsule of immunocompromised mice. After eight weeks, the matured tHIOs were harvested and processed to proliferate into three-dimensional H9tHIEs, following the same protocol used for generating HIEs from human intestinal tissues and biopsies. The resulting H9tHIEs could be passaged indefinitely, and they also are epithelial only cultures without an outer mesenchyme, a morphology similar to tissue stem cell-derived HIEs (37).

We next investigated whether the H9tHIEs would support replication of GII.4

Sydney[P31] and GII.3[P21] HuNoVs. Efficient replication of both GII genotypes was achieved (Figure 2A and 2B). A direct comparison of virus replication in the H9tHIEs and our commonly used lab prototype J2 HIE, used extensively in many studies (9), and J4*FUT2-KI* HIE lines showed that H9tHIEs supported GII.4 replication with no significant difference in viral yield when compared to the J2 and a significant reduction in viral yield when compared to the J4*FUT2-KI* line, respectively. For GII.3, there was a higher viral yield in the H9tHIE line compared to replication in the J2 HIE line, but the best replication was in the J4*FUT2-KI* HIE line. Both HuNoV strains had significant replication increases in J4*FUT-KI* compared to the J2 line.

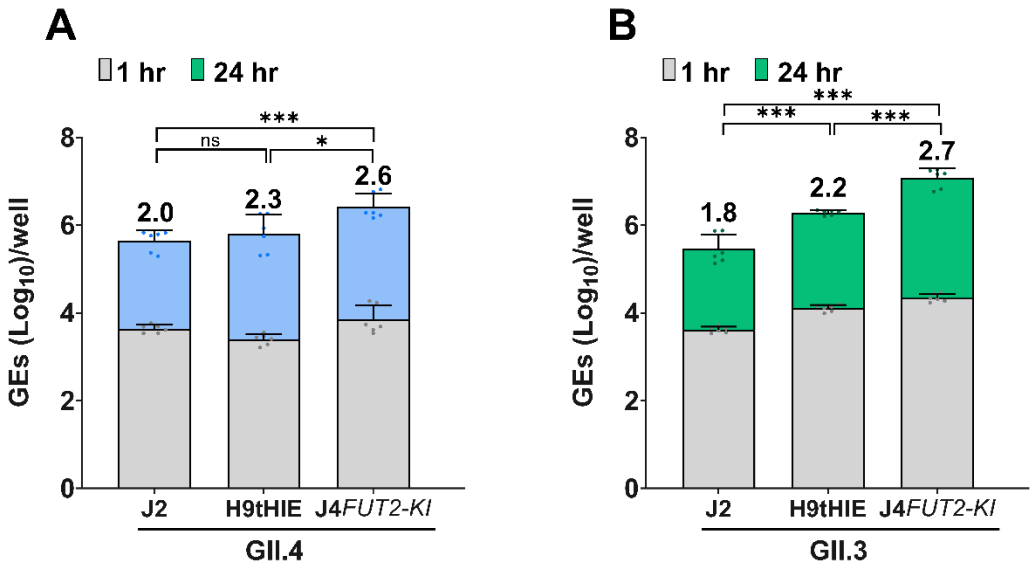

Figure 2: HuNoV replication in H9tHIEs.
Differentiated H9tHIE monolayers in OGM differentiation medium were infected with **(A)** GII.4 Sydney[P31] (9×10^5 GEs/well) or **(B)** GII.3[P21] (4.3×10^5 GEs/well) in presence of 500 µM GCDCA. After 1 hpi, monolayers were washed twice and cultured in OGM differentiation medium (+ 500 µM GCDCA). Values on bars represent the net $\log_{10}$ difference in viral growth (Δ24hr-1hr). Gray shading indicates GE at 1 hpi and blue (A) or green (B) shows GE at 24 hpi. Data from one out of two experiments is shown (n=2). Error bars denote standard deviation , and each data bar represents the mean for three wells of inoculated HIE monolayers. Total RNA extracted from each well was evaluated by RTqPCR in duplicate. Significance was determined using two-way ANOVA with Dunnett multicomparisons test. *** p value < 0.001; ** p < 0.01; * p < 0.05; ns, not significant.

We next evaluated viral replication in an HIE line (D_{201}HIE) generated from a

duodenal biopsy obtained from a patient with common variable immunodeficiency disease (CVID) who had been suffering from chronic GII.6 HuNoV infection for years. We assessed the replication of GII.4, GII.3 and two GII.6 isolates in the differentiated D_{201}HIE line. The GII.6 virus derived from the CVID patient failed to replicate in this D_{201}HIE line (Figure 4), while the D_{201}HIEs supported the replication of GII.4 Sydney[P31] and GII.3[P21] with geometric mean $\log_{10}$(GE) increases of 2.7 and 2.3, respectively. The lack of replication of the patient's own virus was not likely due to the inability of this line to support GII.6 HuNoV replication because a different clinical isolate of GII.6 virus (TCH13-106) from a child hospitalized with acute gastroenteritis showed a minimal replication of 0.6 geometric mean $\log_{10}$ (GE) increase (Figure 3).

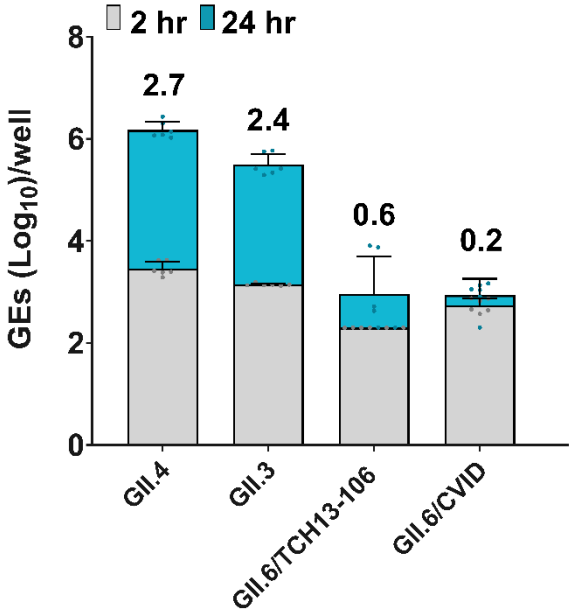

Figure 3: HuNoV replication in D201. D201 HIE monolayers were differentiated in OGM differentiation medium and infected with GII.4/Sydney (9×10^5 GEs/well), GII.3 (4.3×10^5 GEs/well), GII.6/TCH13-106 (3.3×10^5 GEs/well) or GII.6/CVID (9.7×10^4 GEs/well) diluted in CMGF(-) supplemented with 500 µM GCDCA. After 2 hpi, monolayers were washed twice and cultured in OGM differentiation medium (+ 500 µM GCDCA). Values on bars represent net $\log_{10}$ difference in viral growth. Gray shading indicates GE at 1 hpi and blue shows GE at 24 hpi. Data from one out of two experiments is shown (n=2). Error bars denote standard deviation, and each data bar represents the mean for three wells of inoculated HIE monolayers from one representative experiment. Total RNA extracted from each well was evaluated by RTqPCR in duplicate.

We also investigated whether the GII.6 virus inoculum from the CVID patient might not be infectious by testing replication of this virus in three other jejunal HIE lines, including the J2 HIE line and two genetically-modified J2*STAT1-KO* and J4*FUT2-KI* HIE lines made previously (30). The GII.6/CVID patient-derived virus showed minimal or no replication in J2 and J2*STAT1-KO HIEs,* respectively, but it did replicate with a geometric mean $\log_{10}$(GE) increase of 1.3 in the J4*FUT2-KI* HIE (Figure 4A). The other GII.6 isolate (TCH13-106), which replicated minimally in the D_{201}HIE line (Figure 3) was tested as a positive control and showed significant $\log_{10}$(GE) increases in all jejunal HIE lines (Figure 4B).

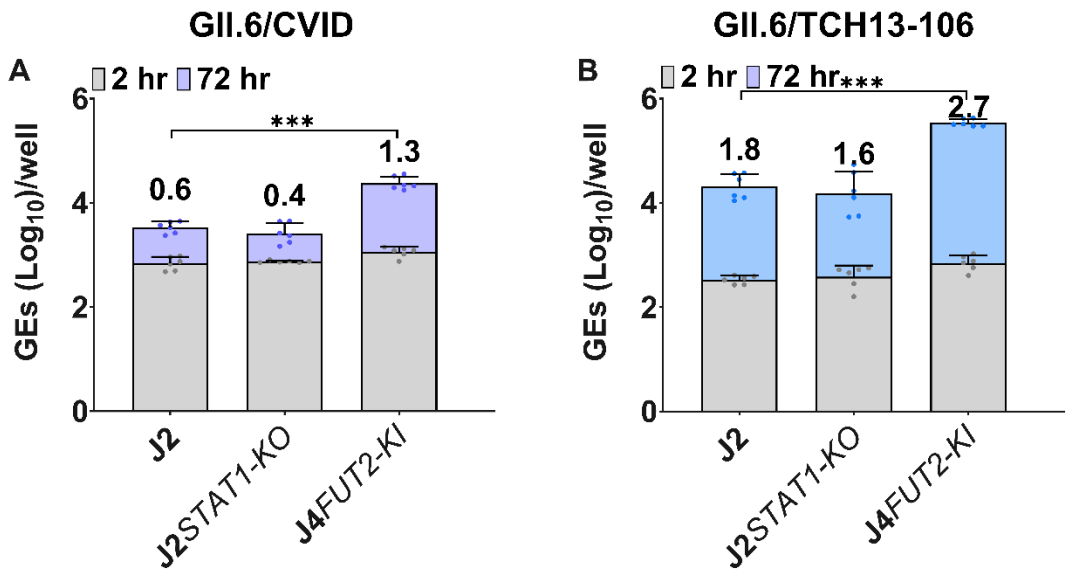

Figure 4: HuNoV replication in genetically modified HIEs.
HIE monolayers were differentiated in OGM differentiation medium and inoculated with **(A)** GII.6/CVID (9.7×10^4 GEs/well) or **(B)** GII.6/TCH13-106 (3.3×10^5 GEs/well) in presence of 500 µM GCDCA. After 1-2 hpi, monolayers were washed twice and cultured in OGM differentiation medium (+ 500 µM GCDCA). Values on bars represent net $\log_{10}$ difference in viral growth. Gray bars indicate GE at 1-2 hpi and colored bars show GE at 72 hpi. *** p value < 0.001. Data from one out of two experiments is shown (n=2). Error bars denote standard deviation, and each data bar represents the mean for three wells of inoculated HIE monolayers from one representative experiment.

Next, we evaluated GII.4 and GII.3 viral replication in jejunal HIE lines (J1005 and J1006) established from specimens collected during surgery from two preterm infants, 37

and 43 weeks corrected gestational age at the time of surgical sample collection, respectively (38). Virus replication in these lines was compared to that in the prototype J2 line and the J4*FUT2-KI* HIE line. The jejunal HIEs from both infants supported replication of these two viruses, with a similar GII.4 replication pattern compared to the prototype J2 and a significant reduction in GII.4 $\log_{10}$(GE) compared to replication in the J4*FUT2-KI* HIE line. There also was significantly less GII.3 replication in the infant lines compared to the adult lines. Nevertheless, both GII.4 and GII.3 strains replicated in all four HIE lines tested (Figure 5).

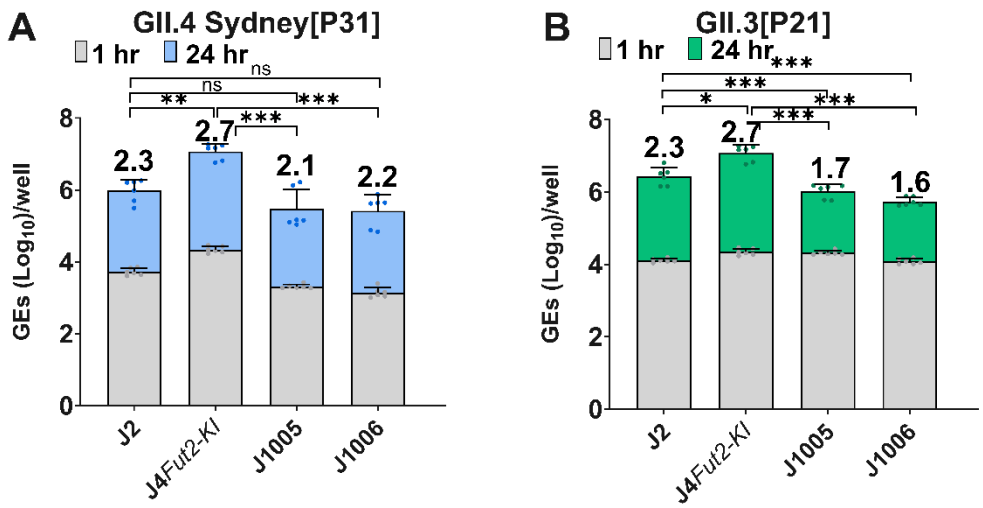

Figure 5: HuNoV replication in HIEs from adults and infants. HIE monolayers were differentiated in OGM differentiation medium and infected with **(A)** GII.4/Sydney (9×10^5 GEs/well) or **(B)** GII.3 (4.3×10^5 GEs/well) diluted in CMGF(-) supplemented with 500 μM GCDCA. After 1 hpi, monolayers were washed twice and cultured in OGM differentiation medium (+ 500 μM GCDCA). Values on bars represent net $\log_{10}$ difference in viral growth (Δ24hr-1hr). Gray bars indicates GE at 1 hpi and colored bars show GE at 24 hpi. *** p value < 0.001; ** p < 0.01; * p < 0.05; ns, not significant. Data from one out of two experiments is shown (n=2). Error bars denote standard deviation, and each data bar represents the mean for three wells of inoculated HIE monolayers.

Finally, we evaluated whether these lines exhibit quantitatively different susceptibilities to infection with the GII.4 and GII.3 viruses by determining the 50% tissue culture infectious dose ($TCID_{50}$) values for each virus for each line. The lowest $TCID_{50}$

was seen for the GII.3 virus in the J4*FUT2-KI* HIE [3.5 (*0.03*)], [log_{10}TCID50 (GE), standard error of the mean (SEM)], followed by the infant HIEs [3.6 (*0.19*) and 3.6 (*0.04*) for J1005 and J1006, respectively]. Surprisingly, the $TCID_{50}$ of GII.4 Sydney[P31] HuNoV was significantly higher in the J4*FUT2-KI* line [4.3 (*0.13*)] compared to J2 [3.9 (*0.12*)] and infant HIEs [3.7 (*0.07*) and 3.7 (*0.1*) for J1005 and J1006, respectively] (Table 2). To explore the specificity of this observed high TCID50 for GII.4, we introduced GII.4 Sydney[P16] (38) into this assay. The TCID50 of this strain reflected the pattern observed for GII.4 Sydney[P31], with elevated TCID50 values particularly seen in the J4*FUT2-KI* line [5.1 (*0.04*)] (Table 2).

Table 2: $TCID_{50}$ [log_{10}(GE)] values of GII.3 and GII.4 in different jejunal HIEs

HIE Line	Adult/Infant	Segment	$TCID_{50}$ (GE)		
			GII.4 Sydney[P31]	GII.4 Sydney[P16]	GII.3[P21]
J2	Adult	Jejunal	3.9 (0.12) *****	4.3 (0.17) ****	3.7 (0.16) ***
J4*FUT2/KI*	Adult	Jejunal	4.3 (0.13) ***	5.1 (0.04) ***	3.5 (0.03) ***
J1005	Infant	Jejunal	3.7 (0.07) *****	3.9 (0.15) ****	3.6 (0.19) ***
J1006	Infant	Jejunal	3.7 (0.10) *****	3.9 (0.16) ****	3.6 (0.04) ***

Differentiated monolayers were inoculated, in six wells per dilution in each experiment, with two-fold dilutions of GII.4 Sydney[P31], GII.4 Sydney[P16], or GII.3[P21]. After 1 hpi, monolayers were washed twice and cultured in the OGM differentiation medium (+ 500 µM GCDCA). Values represent Log_{10}(GE) mean increase in viral growth at 24 hpi from n=3-5 experiments; values in parentheses correspond to SEM (standard error of mean). (*): number of independent experiments.

Building upon our previous investigation where we demonstrated the successful replication of one GI genotype and 11 GII genotypes using the established HuNoV cultivation system (23), the current study demonstrates the capability of J4*FUT2-KI* to support enhanced replication of GII.4, GII.3, and GII.6 HuNoVs, as indicated by the data presented above. Based on these findings, we aimed to further elucidate the replication of additional HuNoV strains in J4*FUT2-KI* HIE monolayers. By using this HIE line in our screening, we expanded the spectrum of cultivatable HuNoV strains to encompass three additional GI genotypes, GI.4, GI.5, and GI.7, and an additional GII.4 Hunter 2004 variant

(Table 3).

Table 3: Cultivated HuNoV genotypes in HIE culture system

Genogroup	Genotype	Reference strain	P Type	Cultivatable strains	Log_{10} increase in viral RNA
GI	GI.1	GI.1[P1]/1968/Norwalk	P1	1	1.9
	GI.4	PCO-1993	P4	1	1.1
	GI.5	PCO-1638	P4	1	0.6
	GI.7	PCO-475	ND	1	0.8
GII	GII.1	TCH18-98	P16	1	1.7
	GII.2	TCH05-951	P2	1	2.1
	GII.3	TCH04-577	P21	2	3.0
		PCO-2061	P12		1.8
	GII.4 Lanzou_2002	TCH02-276	P4	1	0.8
	GII.4 Farmington Hills_2002	TCH04-191	P4	2	2.3
		TCH02-539	ND		0.9
	GII.4 Hunter_2004	TCH05-797	P4	1	1.8
	GII.4 Yerseke_2006a	TCH07-194	P4	3	2.0
		TCH02-186	P4		1.5*
		TCH02-276	P4		0.8*
	GII.4 Den Haag_2006b	TCH07-882	P4	6	2.2
		MDA09-01	P4		2.4
		TCH23-323	P16		2.3
		TCH08-227	P4		1.5*
		TCH08-429	P4		1.3*
		TCH08-430	P4		0.9*
	GII.4 New Orleans_2009	TCH11-64	P4	2	1.7
		TCH23-25	P4		0.9
	GII.4 Sydney_2012	TCH12-580	P31	7	2.7
		TCH14-10	P31		2.0*
		TCH15-82	P31		2.7
		TCH15-88	P31		3.0*
		TCH15-123	P16		2.0*
		BCM16-1	P31		2.0
		BCM16-16	P16		2.2
	GII.4 Sydney_2015	BCM16-22	P16	4	1.8*
		TCH19-76	P16		2.3
		BTH18-10	P16		2.0
		BTH19-9	P16		0.8
	GII.6	TCH13-106	P7	4	1.3
		TCH15-167	P7		2.9
		TCH08-166	P7		1.0*
		CVID	ND		1.3
	GII.7	TCH06-163	P8	1	0.5*
	GII.8	TCH09-279	P7	1	0.7
	GII.12	TCH09-477	P8	1	1.1
	GII.13	TCH10-338	ND	1	0.9
	GII.14	TCH14-364	P16	1	1.5
	GII.17	TCH14-385	P38	2	2.1
		1295-44	P13		1.5

ND, not determined; infections with (*) were performed in in-house media; infections without (*) were performed in OGM media; all infections were conducted in the presence of GCDCA.

Discussion

In our previous work, we reported conditions that enhanced the HIE culture system for HuNoV replication, marked by an expansion in the number of cultivatable strains and increased replication magnitude (23). Since then, we have established several novel HIE lines, prompting us to undertake a new evaluation to ascertain whether any of these newly established lines exhibit better performance for supporting HuNoV replication compared to our existing culture system. Additionally, the introduction of the ODM medium in 2020, by STEMCELL, raised the question about its potential to outperform the OGM media in supporting HuNoV replication.

Our comparative analysis between OGM and ODM media revealed a significant enhancement in the replication efficiency of GII.4 Sydney[P31] and GII.3[P21] with OGM. This comparison, not previously undertaken in other studies that used OGM or ODM media (28, 39-43), provides guidance for laboratories using commercial media for HuNoV studies. Further, an evaluation of newly established lines, derived from intestinal segments of different donors, highlights strain-, donor- and segment-specific differences within the GII genogroup of HuNoVs. Varying viral replication efficiency between different intestinal segments and donors, suggests differences in receptor expression, innate immune responses, or other host factors. More detailed studies of host factors that may be responsible for the segment- and strain-specific differences in susceptibility to HuNoV infection can provide new, valuable insights into the biology and pathogenesis of HuNoV infections. The lack of infection in the colonic HIEs from the same donors, where small intestinal cultures support infection, is consistent with previous histological studies that showed no detection of viral capsid protein in colon biopsies from immunocompromised

patients with chronic HuNoV infection and from our previous replication studies in colonic HIEs generated from biopsies of different donors (23, 44). These new studies exclude genetics as being the factor for the lack of replication in colonic cultures.

Our studies also demonstrate that H9hESC-derived H9tHIEs support HuNoV replication. The H9hESCs are capable of differentiation into various cell types, including enteric neuronal cells or immune cells (45, 46), offering potential applications for future co-culture studies for a more comprehensive human intestinal model. The functional properties of these H9tHIE cultures may align more closely with those of human intestinal stem cell-derived HIEs, since they support efficient replication of HuNoV strains (Figure 2). Direct comparison of HuNoV replication to J2 HIEs showed that H9tHIEs provided higher viral yields, specifically for GII.3[P21]. Future studies are needed to examine their quantitative susceptibility through a comparative assessment of $TCID_{50}$ values across multiple viral strains.

Additionally, the replication data indicate that the J4*FUT2-KI* line supports better HuNoV replication compared to the other HIE lines tested. The GII.6 CVID patient-derived virus exhibited optimal replication in J4*FUT2-KI*, with minimal observed replication in J2, and no replication observed in J2*STAT1-KO* and the patient's own line. The lower titer of this virus, compared to GII.6/TCH13-106, might be a factor contributing to its poor replication. Van Kampen et al. also reported no replication of a CVID patient-derived GII.4 in the J2 line (16). The susceptibility of J4*FUT2-KI* to GII.6 CVID infection remains to be understood, possibly linked to higher HBGA expression or a downregulated immune response. This represents an opportunity to study the biologic properties and viral evolution in a chronically infected host.

Lastly, infant HIE lines (38) exhibited good GII.3 and GII.4 viral yields but did not surpass those in adult J2 and J*4Fut2-KI* HIE lines. Quantitative comparative assessment, based on inoculation of infant and adult HIEs with 100 $TCID_{50}$, revealed the J4*FUT2-KI* HIE line is the most susceptible to GII.3, which is consistent with our previous data (30), while both GII.4 Sydney variants demonstrated higher $TCID_{50}$ in this line. The underlying reason for these differences remains to be determined but they may reflect the different pathways used by GII.4 and GII.3 to enter cells. GII.3 requires bile acid to induce endocytosis while GII.4 uses a rather complex cell wounding and CLIC-mediated pathway (47, 48). These distinct results raise the possibility of previously unrecognized strain-specific differences in susceptibility to viral infection in HIEs based on the host's age but additional HIE lines from infants or younger children will need to be made and tested.

In conclusion, this study significantly advances our understanding of HuNoV infection by confirming viral replication in diverse HIEs, including H9tHIEs, those from a CVID patient, organ donors, and infants. Incorporating HIEs from multiple donors reveals segment-specific susceptibility to HuNoV infection. H9tHIEs effectively mimic the human intestinal environment. We have expanded the spectrum of cultivatable HuNoV strains, demonstrating positive replication for 4 GI and 11 GII genotypes. Ongoing optimization efforts showed strain- and segment-specific differences in replication, enhancing our understanding of HuNoV biology holding valuable implications for antiviral testing and therapeutic discovery.

Material and methods

HIES and viruses

HIE cultures used in this study are from an HIE bank maintained by Gastrointestinal Experimental Model Systems Core (GEMS) of the Texas Medical Center Digestive Diseases Center (TMC DDC) (Table 4). HIEs were generated from distinct intestinal segments from organ donors provided by the organ donation group LifeGift (Houston, TX, USA). Whole intestines were delivered on ice one hour after arrival (49). The intestinal regions were identified as follows: the duodenum was taken from the first 10 cm of the small intestine; jejunum and ileum were separated from the remaining small intestine using the vascularization of the tissue as a guide; the colon region was identified by the morphology of the colon and the patterning of mesenteric fat. Following identification and separation, the intestinal regions were washed with calcium/magnesium-free PBS buffer. HIE cultures were established from small pieces of each intestinal region as previously described (50, 51). The D_{201}HIE line was generated from a duodenal biopsy of an individual with congenital variable immunodeficiency who was chronically infected with human norovirus. H9tHIE line was generated from H9 human Embryonic Stem Cell (H9hESC)-derived HIOs transplanted under kidney capsule of immunocompromised mice. J2*STAT-KO* and J4*FUT2-KI* HIEs are genetically modified and described previously (30). HIEs J1005 and J1006 were generated from two infants, 10 and 12 weeks at surgery (corrected gestational age, 37 and 42 weeks, respectively (38). All HIEs used in this study are secretor positive (see Table 4). Propagation of HIEs as multilobular cultures and preparation of monolayer cultures for infection were performed as previously described

(23). Virus inocula were stool filtrates prepared and stored in aliquots at -80°C as previously described (9).

Table 4: HIE lines used in this study

HIE line	Source age	Phenotyping results		
		Secretor Status	**ABH** Status	**Lewis** Status
J2	52 y	Se+	B	Le^b
$J4^{FUT2/KI}$	62 y	Se+	O	Le^b
LG2002 (D,J,I,C)	34 y	Se+	O	Le^b
LG2003 (D,J,I,C)	23 y	Se+	O	Le^b
LG2004 (D,J,I,C)	25 y	Se+	A	Le^b
LG2005 (D,J,I,C)	23 y	Se+	O	Le^b
H9tHIE	18 wks *	Se+	B	Le^b
J1005	10/37 wks **	Se+	A	Le^b
J1006	12/43 wks **	Se+	B	Le^b
D201	56 y	Se+	O	Le^b

Se, secretor; Le, Lewis; y, years; wks, weeks; D, duodenum; J, jejunum, I, ileum; C, colon; (*): H9tHIE were generated from 8-week-old tHIOs which are developmentally similar to an 18 gestational week human fetal intestine (36); (**): (age at surgery/corrected gestational age at surgery).

Viral infection

Five-day differentiated HIE monolayers were washed once with CMGF(−) medium (9) and inoculated with HuNoV for 1-2 h at 37°C. The inoculum was removed, and monolayers were washed twice with CMGF(−) medium to remove the unbound virus. OGM or ODM differentiation medium [100 µL containing 500 µM bile acid glycochenodeoxycholic acid (GCDCA)] was then added, and the cultures were incubated at 37°C for the indicated time points.

Tissue culture infectious dose 50% ($TCID_{50}$) assay

Four HIE lines from 2 infants (J1005 and J1006) and 2 adults (J4*FUT2/KI*, and the prototype J2) were seeded as monolayers in 96-well plate for 24 hrs in OGM proliferation medium supplemented with 10 μM Rock inhibitor Y-27632, and differentiated for 5 days in OGM differentiation medium by changing the medium every other day. Prior to infection, one aliquot of the GII.4 Sydney[P31] ($1.8x10^7$ GEs/μL), GII.4 Sydney[P16] ($4.3x10^6$ GEs/μL), or GII.3 ($7.4x10^6$ GEs/μL) stool samples was thawed and diluted 1:5,000 in Dulbecco's phosphate buffer saline calcium/magnesium free (DPBS; ThermoFisher). This viral dilution was 2-fold serially diluted in CMGF(-) basal medium supplemented with 500 μM GCDCA bile acid in a 96-well round-bottom plate. Six replicates were typically prepared for each dilution. HIE monolayers were then infected with 100 μL of each dilution for 1 hr at 37°C under 5% CO_2 atmosphere, washed twice with CMGF(-) basal medium, and incubated in 100 μL/well OGM with 500 μM GCDCA. After 24 hpi, total RNA was extracted from each well and viral replication was assessed by RT-qPCR in duplicate using a standard curve based on recombinant HuNoV RNA transcript as described below. The numbers of infected wells that yielded a positive signal by RT-qPCR were counted. PCR wells that showed values greater than the limit of detection (LOD = 20 GEs) were considered as positive and wells with values less than 20 were considered negative (no infection). The $TCID_{50}$ was calculated by the Reed-Muench method. Compiled data from 3-5 different experiments were presented.

Quantification of viral replication by RT-qPCR

RNA extraction and RT-qPCR were performed as previously described (23). In brief, total RNA was extracted from each infected well using the KingFisher Flex purification system

and MagMAX-96 Viral RNA isolation kit. RNA extracted at 1 hpi was used as a baseline to determine the amount of input virus that remained associated with cells after washing the infected cultures to remove unbound virus. The primer pair and probe COG2R/QNIF2d/QNIFS (52) were used in the RT-qPCR for detection of GII genotypes and the primer pair and probe NIFG1F/V1LCR/NIFG1P (53) were used for GI.1. RT-qPCR was performed with qScript XLT One-Step RT-qPCR ToughMix reagent with ROX reference dye (Quanta Biosciences) in an Applied Biosystems StepOnePlus thermocycler. Each extracted RNA was run in duplicate with the cycling conditions: 50°C (15 min), 95°C (5 min), followed by 40 cycles of 95°C (15 s) and 60°C (35 s). Standard curves based on recombinant GII HuNoV RNA transcripts were used to quantitate viral genome equivalents (GEs) in RNA samples. The limit of detection of the RT-qPCR assay was 20 GEs. A threshold for successful viral replication was established by considering a 0.5 increase in $\log_{10}$(GE) after 24 hpi relative to the genomic RNA detected at 1 hpi (23).

Statistical analysis

Each experiment was performed more than once, with three technical replicates of each culture condition and time point. Compiled data from at least two experiments was presented. All statistical analyses were performed on GraphPad Prism version 9.0 for Windows (GraphPad Software, La Jolla, CA, USA). Samples with RNA levels below the limit of detection of the RT-qPCR assay were assigned a value that was one-half the limit of detection of the assay (LOD = 20). Comparison between groups was performed using the two-way ANOVA with Dunnet multicomparisons test. P values of <0.05 were

considered statistically significant.

Data availability

All data are available in the paper. All HIE cultures used in this study are from an HIE bank maintained by the Texas Medical Center Digestive Diseases Center (TMC DDC) core https://www.bcm.edu/research/research-centers/texas-medical-center-digestive-diseases-center.

Acknowledgements

This work was funded in part by Public Health Service grant P01-AI057788 to M.K.E, R.L.A., and BVV Prasad, P30 DK 056338 (to H. El-Serag), which supports the Texas Medical Center Digestive Diseases Center and GEMS Core, and NIH 1K08DK131326 to A.L.S. The authors acknowledge the Advanced Technology Core Laboratories (Baylor College of Medicine), specifically the Integrated Microscopy Core with funding from the NIH (DK56338, CA125123, ES030285), and 398 CPRIT (RP150578, RP170719). We thank LifeGift, Javier Nieto, and the donor families for providing intestines for generating HIEs.

References

1. Atmar, R.L., S. Ramani, and M.K. Estes, *Human noroviruses: recent advances in a 50-year history.* Curr Opin Infect Dis, 2018. **31**(5): p. 422-432.
2. de Graaf, M., J. van Beek, and M.P.G. Koopmans, *Human norovirus transmission and evolution in a changing world.* Nature Reviews Microbiology, 2016. **14**(7): p. 421-433.
3. Green, K.Y., *Norovirus infection in immunocompromised hosts.* Clin Microbiol Infect, 2014. **20**(8): p. 717-23.
4. Pires, S.M., et al., *Aetiology-Specific Estimates of the Global and Regional Incidence and Mortality of Diarrhoeal Diseases Commonly Transmitted through Food.* PLoS One, 2015. **10**(12): p. e0142927.
5. Bartsch, S.M., et al., *Global Economic Burden of Norovirus Gastroenteritis.* PLoS One, 2016. **11**(4): p. e0151219.
6. Bartsch, S.M., K.J. O'Shea, and B.Y. Lee, *The Clinical and Economic Burden of Norovirus Gastroenteritis in the United States.* J Infect Dis, 2020. **222**(11): p. 1910-1919.
7. Debbink, K., L.C. Lindesmith, and R.S. Baric, *The state of norovirus vaccines.* Clin Infect Dis, 2014. **58**(12): p. 1746-52.
8. Prasad, B.V., et al., *Antiviral targets of human noroviruses.* Curr Opin Virol, 2016. **18**: p. 117-25.
9. Ettayebi, K., et al., *Replication of human noroviruses in stem cell-derived human enteroids.* Science, 2016. **353**(6306): p. 1387-1393.
10. Alvarado, G., et al., *Broadly cross-reactive human antibodies that inhibit genogroup I and II noroviruses.* Nat Commun, 2021. **12**(1): p. 4320.
11. Ettayebi, K., et al., *Antiviral Activity of Olanexidine-Containing Hand Rub against Human Noroviruses.* mBio, 2022. **13**(2): p. e0284821.
12. Alvarado, G., et al., *Human Monoclonal Antibodies That Neutralize Pandemic GII.4 Noroviruses.* Gastroenterology, 2018. **155**(6): p. 1898-1907.
13. Atmar, R.L., et al., *Comparison of Microneutralization and Histo-Blood Group Antigen-Blocking Assays for Functional Norovirus Antibody Detection.* J Infect Dis, 2020. **221**(5): p. 739-743.
14. Costantini, V., et al., *Human Norovirus Replication in Human Intestinal Enteroids as Model to Evaluate Virus Inactivation.* Emerg Infect Dis, 2018. **24**(8): p. 1453-1464.
15. Lewis, M.A., et al., *Standardization of an antiviral pipeline for human norovirus in human intestinal enteroids demonstrates nitazoxanide has no to weak antiviral activity.* Antimicrob Agents Chemother, 2023. **67**(10): p. e0063623.
16. van Kampen, J.J.A., et al., *Clinical and In Vitro Evidence Favoring Immunoglobulin Treatment of a Chronic Norovirus Infection in a Patient With Common Variable Immunodeficiency.* J Infect Dis, 2022. **226**(10): p. 1781-1789.
17. Salmen, W., et al., *A single nanobody neutralizes multiple epochally evolving human noroviruses by modulating capsid plasticity.* Nat Commun, 2023. **14**(1): p. 6516.
18. Hayashi, T., et al., *Dasabuvir Inhibits Human Norovirus Infection in Human Intestinal Enteroids.* mSphere, 2021. **6**(6): p. e0062321.

19. Mirabelli, C., et al., *Human Norovirus Efficiently Replicates in Differentiated 3D-Human Intestinal Enteroids.* J Virol, 2022. **96**(22): p. e0085522.
20. Ford-Siltz, L.A., et al., *Cross-reactive neutralizing human monoclonal antibodies mapping to variable antigenic sites on the norovirus major capsid protein.* Front Immunol, 2022. **13**: p. 1040836.
21. Lindesmith, L.C., et al., *Sera Antibody Repertoire Analyses Reveal Mechanisms of Broad and Pandemic Strain Neutralizing Responses after Human Norovirus Vaccination.* Immunity, 2019. **50**(6): p. 1530-1541.e8.
22. Koromyslova, A.D., et al., *Human Norovirus Neutralized by a Monoclonal Antibody Targeting the Histo-Blood Group Antigen Pocket.* J Virol, 2019. **93**(5).
23. Ettayebi, K., et al., *New Insights and Enhanced Human Norovirus Cultivation in Human Intestinal Enteroids.* mSphere, 2021. **6**(1).
24. Atmar, R.L., et al., *A Bivalent Human Norovirus Vaccine Induces Homotypic and Heterotypic Neutralizing Antibodies.* J Infect Dis, 2023.
25. Mboko, W.P., et al., *Advances in understanding of the innate immune response to human norovirus infection using organoid models.* J Gen Virol, 2022. **103**(1).
26. Chan, J.C.M., et al., *Targeted Profiling of Immunological Genes during Norovirus Replication in Human Intestinal Enteroids.* Viruses, 2021. **13**(2).
27. Hosmillo, M., et al., *Norovirus Replication in Human Intestinal Epithelial Cells Is Restricted by the Interferon-Induced JAK/STAT Signaling Pathway and RNA Polymerase II-Mediated Transcriptional Responses.* mBio, 2020. **11**(2).
28. Hayashi, T., et al., *Inhibitory effect of Ephedra herba on human norovirus infection in human intestinal organoids.* Biochem Biophys Res Commun, 2023. **671**: p. 200-204.
29. Carmona-Vicente, N., et al., *Human intestinal enteroids platform to assess the infectivity of gastroenteritis viruses in wastewater.* Water Res, 2024. **255**: p. 121481.
30. Haga, K., et al., *Genetic Manipulation of Human Intestinal Enteroids Demonstrates the Necessity of a Functional Fucosyltransferase 2 Gene for Secretor-Dependent Human Norovirus Infection.* mBio, 2020. **11**(2).
31. Spence, J.R., et al., *Directed differentiation of human pluripotent stem cells into intestinal tissue in vitro.* Nature, 2011. **470**(7332): p. 105-9.
32. Finkbeiner, S.R., et al., *Transcriptome-wide Analysis Reveals Hallmarks of Human Intestine Development and Maturation In Vitro and In Vivo.* Stem Cell Reports, 2015. **4**(6): p. 1140-55.
33. Boyle, M.A., et al., *In Vivo Transplantation of Human Intestinal Organoids Enhances Select Tight Junction Gene Expression.* J Surg Res, 2021. **259**: p. 500-508.
34. Bouffi, C., et al., *In vivo development of immune tissue in human intestinal organoids transplanted into humanized mice.* Nat Biotechnol, 2023.
35. Watson, C.L., et al., *An in vivo model of human small intestine using pluripotent stem cells.* Nat Med, 2014. **20**(11): p. 1310-4.
36. Singh, A., et al., *Transplanted human intestinal organoids: a resource for modeling human intestinal development.* Development, 2023. **150**(9).
37. Sato, T., et al., *Single Lgr5 stem cells build crypt-villus structures in vitro without a mesenchymal niche.* Nature, 2009. **459**(7244): p. 262-5.

38. Adeniyi-Ipadeola, G.O., et al., *Infant and Adult Human Intestinal Enteroids are Morphologically and Functionally Distinct.* bioRxiv, 2023.
39. Hayashi, T., et al., *Evaluation of Heat Inactivation of Human Norovirus in Freshwater Clams Using Human Intestinal Enteroids.* Viruses, 2022. **14**(5).
40. Euller-Nicolas, G., et al., *Human Sapovirus Replication in Human Intestinal Enteroids.* J Virol, 2023. **97**(4): p. e0038323.
41. Narwankar, R. and M.A. Esseili, *Replication of Human Norovirus in Human Intestinal Enteroids Is Affected by Fecal Sample Processing.* Viruses, 2024. **16**(2).
42. Santos-Ferreira, N., et al., *Molnupiravir inhibits human norovirus and rotavirus replication in 3D human intestinal enteroids.* Antiviral Res, 2024. **223**: p. 105839.
43. Tenge, V., et al., *Bile acid-sensitive human norovirus strains are susceptible to sphingosine-1-phosphate receptor 2 inhibition.* bioRxiv, 2024.
44. Karandikar, U.C., et al., *Detection of human norovirus in intestinal biopsies from immunocompromised transplant patients.* J Gen Virol, 2016. **97**(9): p. 2291-2300.
45. Workman, M.J., et al., *Engineered human pluripotent-stem-cell-derived intestinal tissues with a functional enteric nervous system.* Nat Med, 2017. **23**(1): p. 49-59.
46. Estridge, R.C., J.E. O'Neill, and A.J. Keung, *Matrigel Tunes H9 Stem Cell-Derived Human Cerebral Organoid Development.* Organoids, 2023. **2**(4): p. 165-176.
47. Ayyar, B.V., et al., *CLIC and membrane wound repair pathways enable pandemic norovirus entry and infection.* Nat Commun, 2023. **14**(1): p. 1148.
48. Murakami, K., et al., *Bile acids and ceramide overcome the entry restriction for GII.3 human norovirus replication in human intestinal enteroids.* Proc Natl Acad Sci U S A, 2020. **117**(3): p. 1700-1710.
49. Danhof, H.A., et al., *Microbial stimulation of oxytocin release from the intestinal epithelium via secretin signaling.* bioRxiv, 2023.
50. Zou, W.Y., et al., *Human Intestinal Enteroids: New Models to Study Gastrointestinal Virus Infections.* Methods Mol Biol, 2019. **1576**: p. 229-247.
51. Sato, T., et al., *Long-term expansion of epithelial organoids from human colon, adenoma, adenocarcinoma, and Barrett's epithelium.* Gastroenterology, 2011. **141**(5): p. 1762-72.
52. Loisy, F., et al., *Real-time RT-PCR for norovirus screening in shellfish.* J Virol Methods, 2005. **123**(1): p. 1-7.
53. Miura, T., et al., *Environmental detection of genogroup I, II, and IV noroviruses by using a generic real-time reverse transcription-PCR assay.* Appl Environ Microbiol, 2013. **79**(21): p. 6585-92.

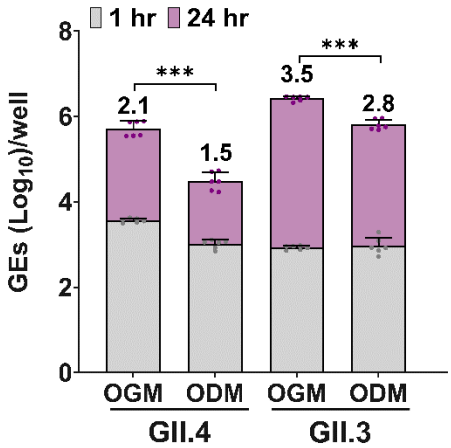

Figure 1: HuNoV replication is enhanced in HIEs plated in OGM compared to ODM media. 3D J4*FUT2/KI* HIEs were propagated in WRNE media. Monolayers were seeded in OGM proliferation medium with ROCK inhibitor and differentiated in OGM or ODM differentiation media. Differentiated monolayers were inoculated with GII.4 Sydney[P31] (9×10^5 GEs/well) or GII.3[P21] (4.3×10^5 GEs/well) diluted in CMGF(-) with 500 μM GCDCA. After 1 hpi, monolayers were washed twice and cultured in the OGM or ODM differentiation media (+ 500 μM GCDCA). Values on bars represent net $\log_{10}$ difference in viral growth (Δ24hr-1hr) preformed in triplicate. Gray shading indicates GE at 1 hpi and purple shows GE at 24 hpi. Asterisks indicate significant difference at 24 hpi between culture conditions. Error bars denote standard deviation (n=2). Data from one out of two experiments is presented. Each data bar corresponds to the mean derived from three wells of inoculated HIE monolayers. Total RNA extracted from each well was evaluated by RTqPCR in duplicate. *** p value < 0.001.

Table 1: HuNoV replication in HIEs from four donors

	GII.4 / Sydney				GII.3			
HIEs	2002	2003	2004	2005	2002	2003	2004	2005
Duodenal	1.3 (*0.9-1.5*)	1.6 (*1.4-1.8*)	2.0 (*1.8-2.1*)	1.8 (*1.7-1.9*)	0.8 (*0.5-1.1*)	0	1.6 (*1.2-1.8*)	0.8 (*0.5-1.1*)
Jejunal	2.2 (*1.9-2.5*)	2.1 (*1.9-2.3*)	1.8 (*1.5-2.0*)	2.1 (*1.9-2.2*)	2.0 (*1.9-2.1*)	0	1.8 (*1.4-2.1*)	1.2 (*0.8-1.6*)
Ileal	2.2 (*2.1-2.4*)	2.2 (*2.1-2.4*)	1.6 (*1.5-1.9*)	2.7 (*2.5-2.8*)	1.8 (*1.4-2.2*)	0.1	1.4 (*1.2-1.6*)	0.5 (*0.3-0.8*)
Colonic	0	0	0	0	0	0	0	0

Differentiated monolayers were inoculated with GII.4 Sydney[P31] (9×10^5 GEs/well) or GII.3[P21] (4.3×10^5 GEs/well) diluted in CMGF(-) with 500 µM GCDCA. After 1 hpi, monolayers were washed twice and cultured in the OGM differentiation medium (+ 500 µM GCDCA). Values represent compiled data of net $\log_{10}$ geometric mean increase in viral growth (Δ24hpi-1hpi) from 3 experiments and six replicates. in each experiment; values in parentheses correspond to 95% confidence interval (95% CI).

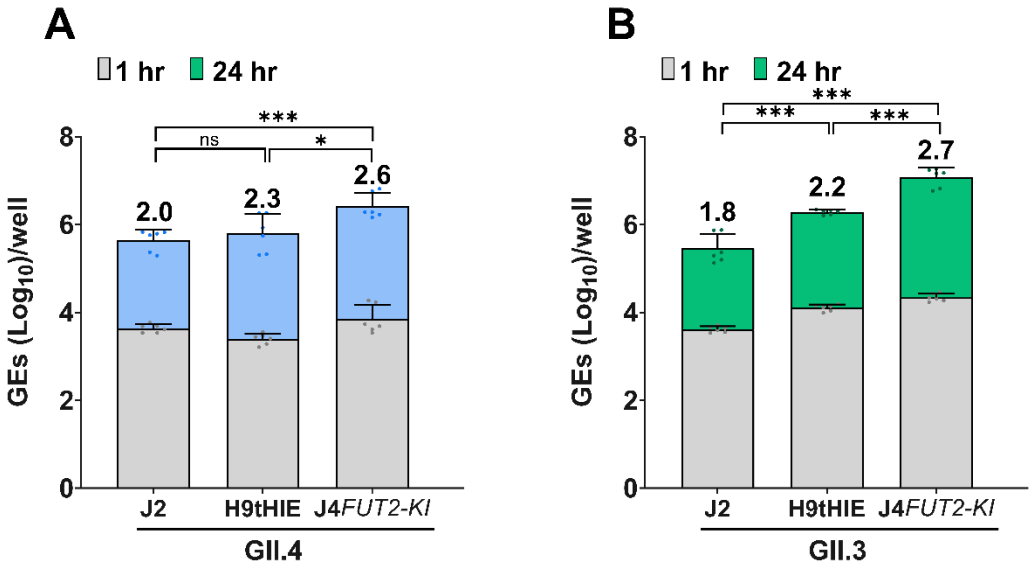

Figure 2: HuNoV replication in H9tHIEs.
Differentiated H9tHIE monolayers in OGM differentiation medium were infected with **(A)** GII.4 Sydney[P31] (9×10^5 GEs/well) or **(B)** GII.3[P21] (4.3×10^5 GEs/well) in presence of 500 µM GCDCA. After 1 hpi, monolayers were washed twice and cultured in OGM differentiation medium (+ 500 µM GCDCA). Values on bars represent the net $\log_{10}$ difference in viral growth (Δ24hr-1hr). Gray shading indicates GE at 1 hpi and blue (A) or green (B) shows GE at 24 hpi. Data from one out of two experiments is shown (n=2). Error bars denote standard deviation , and each data bar represents the mean for three wells of inoculated HIE monolayers. Total RNA extracted from each well was evaluated by RTqPCR in duplicate. Significance was determined using two-way ANOVA with Dunnett multicomparisons test. *** p value < 0.001; ** p < 0.01; * p < 0.05; ns, not significant.

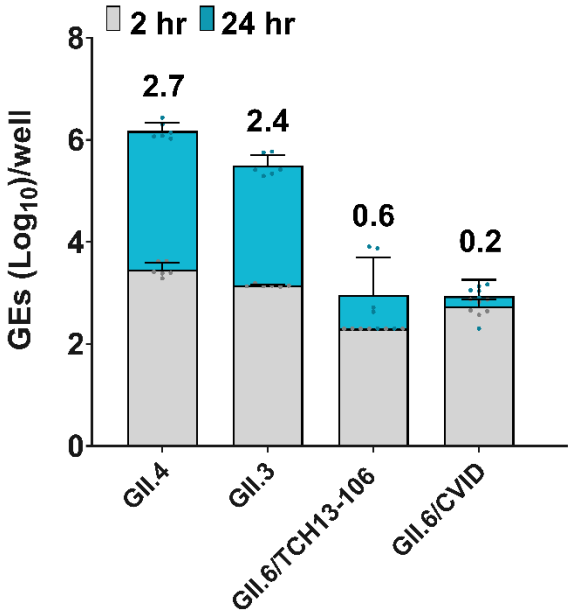

Figure 3: HuNoV replication in D201. D201 HIE monolayers were differentiated in OGM differentiation medium and infected with GII.4/Sydney (9×10^5 GEs/well), GII.3 (4.3×10^5 GEs/well), GII.6/TCH13-106 (3.3×10^5 GEs/well) or GII.6/CVID (9.7×10^4 GEs/well) diluted in CMGF(-) supplemented with 500 µM GCDCA. After 2 hpi, monolayers were washed twice and cultured in OGM differentiation medium (+ 500 µM GCDCA). Values on bars represent net $\log_{10}$ difference in viral growth. Gray shading indicates GE at 1 hpi and blue shows GE at 24 hpi. Data from one out of two experiments is shown (n=2). Error bars denote standard deviation, and each data bar represents the mean for three wells of inoculated HIE monolayers from one representative experiment. Total RNA extracted from each well was evaluated by RTqPCR in duplicate.

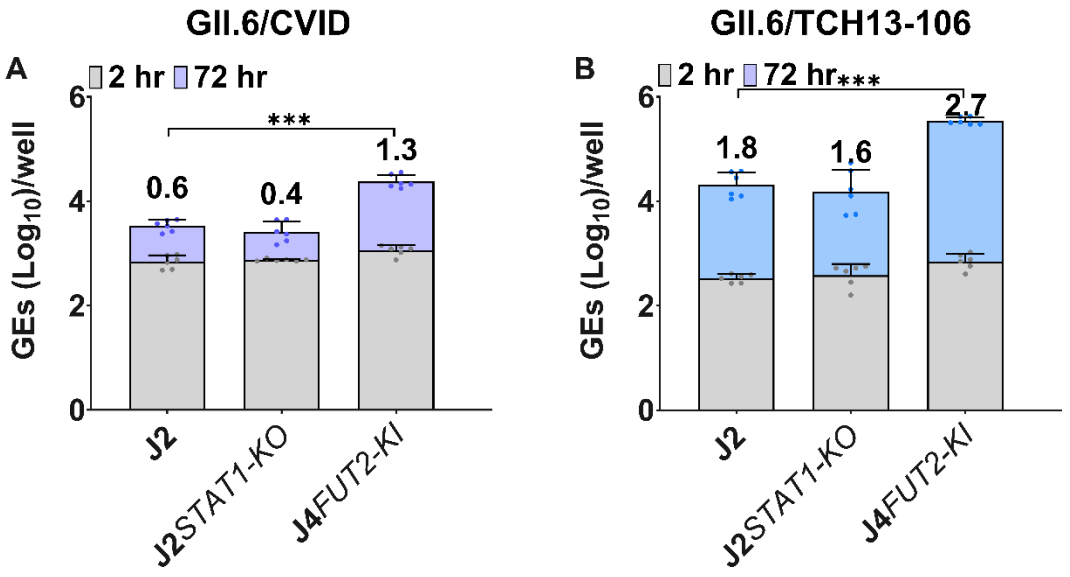

Figure 4: HuNoV replication in genetically modified HIEs.
HIE monolayers were differentiated in OGM differentiation medium and inoculated with **(A)** GII.6/CVID (9.7×10^4 GEs/well) or **(B)** GII.6/TCH13-106 (3.3×10^5 GEs/well) in presence of 500 μM GCDCA. After 1-2 hpi, monolayers were washed twice and cultured in OGM differentiation medium (+ 500 μM GCDCA). Values on bars represent net $\log_{10}$ difference in viral growth. Gray bars indicate GE at 1-2 hpi and colored bars show GE at 72 hpi. *** p value < 0.001. Data from one out of two experiments is shown (n=2). Error bars denote standard deviation, and each data bar represents the mean for three wells of inoculated HIE monolayers from one representative experiment.

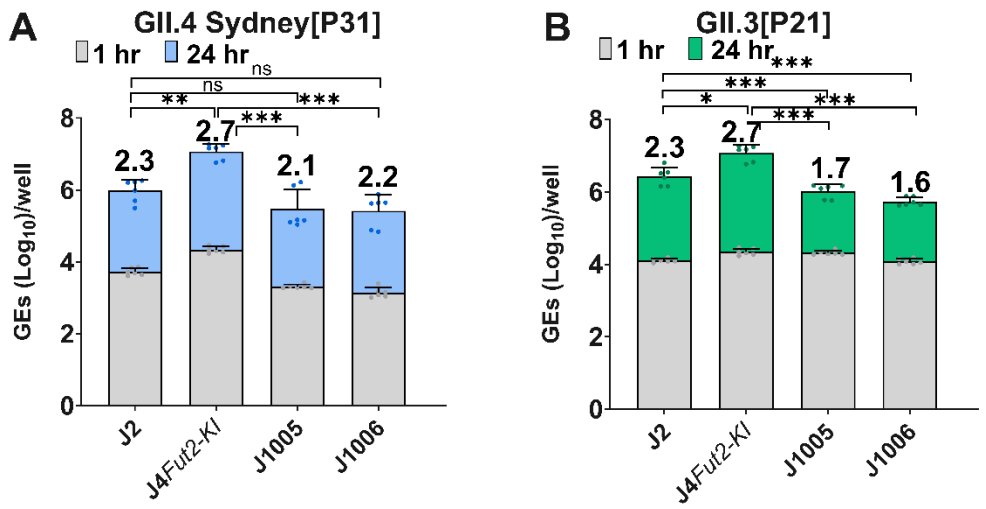

Figure 5: HuNoV replication in HIEs from adults and infants. HIE monolayers were differentiated in OGM differentiation medium and infected with **(A)** GII.4/Sydney (9×10^5 GEs/well) or **(B)** GII.3 (4.3×10^5 GEs/well) diluted in CMGF(-) supplemented with 500 μM GCDCA. After 1 hpi, monolayers were washed twice and cultured in OGM differentiation medium (+ 500 μM GCDCA). Values on bars represent net $\log_{10}$ difference in viral growth (Δ24hr-1hr). Gray bars indicates GE at 1 hpi and colored bars show GE at 24 hpi. *** p value < 0.001; ** p < 0.01; * p < 0.05; ns, not significant. Data from one out of two experiments is shown (n=2). Error bars denote standard deviation, and each data bar represents the mean for three wells of inoculated HIE monolayers.

Table 2: $TCID_{50}$ [log_{10}(GE)] values of GII.3 and GII.4 in different jejunal HIEs

HIE Line	Adult/Infant	Segment	$TCID_{50}$ (GE)		
			GII.4 Sydney[P31]	GII.4 Sydney[P16]	GII.3[P21]
J2	Adult	Jejunal	3.9 (0.12) *****	4.3 (0.17) ****	3.7 (0.16) ***
J4*FUT2/KI*	Adult	Jejunal	4.3 (0.13) ***	5.1 (0.04) ***	3.5 (0.03) ***
J1005	Infant	Jejunal	3.7 (0.07) *****	3.9 (0.15) ****	3.6 (0.19) ***
J1006	Infant	Jejunal	3.7 (0.10) *****	3.9 (0.16) ****	3.6 (0.04) ***

Differentiated monolayers were inoculated, in six wells per dilution in each experiment, with two-fold dilutions of GII.4 Sydney[P31], GII.4 Sydney[P16], or GII.3[P21]. After 1 hpi, monolayers were washed twice and cultured in the OGM differentiation medium (+ 500 µM GCDCA). Values represent Log_{10}(GE) mean increase in viral growth at 24 hpi from n=3-5 experiments; values in parentheses correspond to SEM (standard error of mean). (*): number of independent experiments.

Table 3: Cultivated HuNoV genotypes in HIE culture system

Genogroup	Genotype	Reference strain	P Type	Cultivatable strains	Log_{10} increase in viral RNA
GI	GI.1	GI.1[P1]/1968/Norwalk	P1	1	1.9
	GI.4	PCO-1993	P4	1	1.1
	GI.5	PCO-1638	P4	1	0.6
	GI.7	PCO-475	ND	1	0.8
GII	GII.1	TCH18-98	P16	1	1.7
	GII.2	TCH05-951	P2	1	2.1
	GII.3	TCH04-577	P21	2	3.0
		PCO-2061	P12		1.8
	GII.4 Lanzou_2002	TCH02-276	P4	1	0.8
	GII.4 Farmington Hills_2002	TCH04-191	P4	2	2.3
		TCH02-539	ND		0.9
	GII.4 Hunter_2004	TCH05-797	P4	1	1.8
	GII.4 Yerseke_2006a	TCH07-194	P4	3	2.0
		TCH02-186	P4		1.5*
		TCH02-276	P4		0.8*
	GII.4 Den Haag_2006b	TCH07-882	P4	6	2.2
		MDA09-01	P4		2.4
		TCH23-323	P16		2.3
		TCH08-227	P4		1.5*
		TCH08-429	P4		1.3*
		TCH08-430	P4		0.9*
	GII.4 New Orleans_2009	TCH11-64	P4	2	1.7
		TCH23-25	P4		0.9
	GII.4 Sydney_2012	TCH12-580	P31	7	2.7
		TCH14-10	P31		2.0*
		TCH15-82	P31		2.7
		TCH15-88	P31		3.0*
		TCH15-123	P16		2.0*
		BCM16-1	P31		2.0
		BCM16-16	P16		2.2
	GII.4 Sydney_2015	BCM16-22	P16	4	1.8*
		TCH19-76	P16		2.3
		BTH18-10	P16		2.0
		BTH19-9	P16		0.8
	GII.6	TCH13-106	P7	4	1.3
		TCH15-167	P7		2.9
		TCH08-166	P7		1.0*
		CVID	ND		1.3
	GII.7	TCH06-163	P8	1	0.5*
	GII.8	TCH09-279	P7	1	0.7
	GII.12	TCH09-477	P8	1	1.1
	GII.13	TCH10-338	ND	1	0.9
	GII.14	TCH14-364	P16	1	1.5
	GII.17	TCH14-385	P38	2	2.1
		1295-44	P13		1.5

ND, not determined; infections with (*) were performed in in-house media; infections without (*) were performed in OGM media; all infections were conducted in the presence of GCDCA.

Table 4: HIE lines used in this study

HIE line	Source age	Phenotyping results		
		Secretor Status	**ABH** Status	**Lewis** Status
J2	52 y	Se+	B	Le^b
$J4^{FUT2/KI}$	62 y	Se+	O	Le^b
LG2002 (D,J,I,C)	34 y	Se+	O	Le^b
LG2003 (D,J,I,C)	23 y	Se+	O	Le^b
LG2004 (D,J,I,C)	25 y	Se+	A	Le^b
LG2005 (D,J,I,C)	23 y	Se+	O	Le^b
H9tHIE	18 wks *	Se+	B	Le^b
J1005	10/37 wks **	Se+	A	Le^b
J1006	12/43 wks **	Se+	B	Le^b
D201	56 y	Se+	O	Le^b

Se, secretor; Le, Lewis; y, years; wks, weeks; D, duodenum; J, jejunum, I, ileum; C, colon; (*): H9tHIE were generated from 8-week-old tHIOs which are developmentally similar to an 18 gestational week human fetal intestine (36); (**): (age at surgery/corrected gestational age at surgery).